ORGANIC LETTERS

2010
Vol. 12, No. 8
1728−1731

pH-Controlled Intramolecular Charge-Transfer Behavior in Bistable [3]Rotaxane

Qiao Jiang, Heng-Yi Zhang, Min Han, Zhi-Jun Ding, and Yu Liu*

Department of Chemistry, State Key Laboratory of Elemento-Organic Chemistry, Nankai University, Tianjin 300071, People' Republic of China

yuliu@nankai.edu.cn

Received February 6, 2010

ABSTRACT

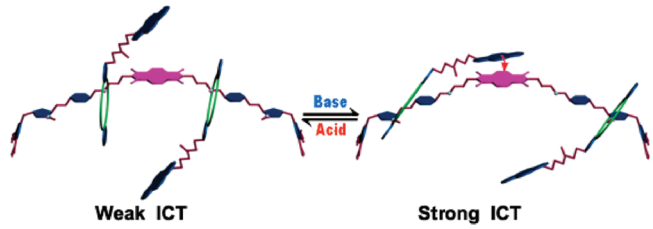

Two [3]rotaxanes with an electron-rich pyrene moiety at the wheel and an electron-deficient naphthalenediimide (NDI) unit in the middle of the axle were prepared through "click chemistry", in which the intramolecular charge-transfer (ICT) process occurred between the pyrene moiety and the NDI unit, and the addition of acid and/or base can adjust the intensity of ICT.

Mechanically interlocked molecules, including rotaxanes and catenanes,[1] have become typical candidates in the design of artificial molecular machines during the past decade owing to their ability to reversibly switch between different states under various external stimuli. They have potential for creating organized, functioning molecular-scale devices which are able to interpret, store, process, and dispatch information just like the sophisticated machines found in natural systems. By employing the stimuli,[1b,d,2] such as illumination,[3] electrochemical potential,[4] pH changes, and ions,[5] chemists can adjust relative positions of the components in interlocked molecules to induce conformational motions and construct various artificial molecular machines like molecular shuttles,[4b,e,5a,6] molecular muscles,[7] molecular elevators,[8] molecular motors,[1e,9] molecular information ratchet,[10] and so on. The varying photophysical properties during their conformational motions are significant, especially for performing their functions.

The bistable rotaxane[3a,4e,8,11] is an important prototype of artifical molecular machines. Bistable [3]rotaxanes[7b] and

(1) (a) Amabilino, D. B.; Stoddart, J. F. *Chem. Rev.* **1995**, *95*, 2725–2828. (b) Balzani, V.; Credi, A.; Raymo, F. M.; Stoddart, J. F. *Angew. Chem., Int. Ed.* **2000**, *39*, 3348–3391. (c) Stoddart, J. F. *Acc. Chem. Res.* **2001**, *34*, 409–522. (d) Balzani, V.; Credi, A.; Venturi, M. *Molecular Devices and Machines: A Journey into the Nanoworld*; Wiley-VCH: Weinheim, Germany, 2003. (e) Kay, E. R.; Leigh, D. A.; Zerbetto, F. *Angew. Chem., Int. Ed.* **2007**, *46*, 72–191. (f) Credi, A.; Tian, H. *Adv. Funct. Mater.* **2007**, *17*, 671–840. (g) Tian, H.; Wang, Q.-C. *Chem. Soc. Rev.* **2006**, *35*, 361–374.

(2) Ballardini, R.; Balzani, V.; Credi, A.; Gandolfi, M. T.; Venturi, M. *Acc. Chem. Res.* **2001**, *34*, 445–455.

(3) (a) Saha, S.; Stoddart, J. F. *Chem. Soc. Rev.* **2007**, *36*, 77–92. (b) Balzani, V.; Credi, A.; Venturi, M. *Chem. Soc. Rev.* **2009**, *38*, 1542–1550. (c) Ma, X.; Tian, H. *Chem. Soc. Rev.* **2010**, *39*, 70–80.

(4) (a) Collier, C. P.; Mattersteig, G.; Wong, E. W.; Luo, Y.; Beverly, K.; Sampaio, J.; Raymo, F. M.; Stoddart, J. F.; Heath, J. R. *Science* **2000**, *289*, 1172–1175. (b) Altieri, A.; Gatti, F. G.; Kay, E. R.; Leigh, D. A.; Martel, D.; Paolucci, F.; Slawin, A. M. Z.; Wong, J. K. Y. *J. Am. Chem. Soc.* **2003**, *125*, 8644–8654. (c) Sobransingh, D.; Kaifer, A. E. *Org. Lett.* **2006**, *8*, 3247–3250. (d) Zou, D.; Andersson, S.; Zhang, R.; Sun, S.; Åkermark, B.; Sun, L. *Chem. Commun.* **2007**, 4734–4736. (e) Fioravanti, G.; Haraszkiewicz, N.; Kay, E. R.; Mendoza, S. M.; Bruno, C.; Marcaccio, M.; Wiering, P. G.; Paolucci, F.; Rudolf, P.; Brouwer, A. M.; Leigh, D. A. *J. Am. Chem. Soc.* **2008**, *130*, 2593–2601.

(5) (a) Ashton, P. R.; Ballardini, R.; Balzani, V.; Baxter, I.; Credi, A.; Fyfe, M. C. T.; Gandolfi, M. T.; Gómez-López, M.; Martínez-Díaz, M.-V.; Piersanti, A.; Spencer, N.; Stoddart, J. F.; Venturi, M.; White, A. J. P.; Williams, D. J. *J. Am. Chem. Soc.* **1998**, *120*, 11932–11942. (b) Keaveney, C. M.; Leigh, D. A. *Angew. Chem., Int. Ed.* **2004**, *43*, 1222–1224. (c) Sindelar, V.; Silvi, S.; Kaifer, A. E. *Chem. Commun.* **2006**, 2185–2187. (d) Huang, Y.-L.; Hung, W.-C.; Lai, C.-C.; Liu, Y.-H.; Peng, S.-M.; Chiu, S.-H. *Angew. Chem., Int. Ed.* **2007**, *46*, 6629–6633. (e) Lankshear, M. D.; Beer, P. D. *Acc. Chem. Res.* **2007**, *40*, 657–668.

10.1021/ol100321k
Published on Web 03/17/2010

bistable [4]rotaxanes,[8,11d] which can be considered as two or three bistable [2]rotaxanes, give us new understanding of applications of bistable [2]rotaxanes in surface chemistry. We recently reported the molecular keypad locks based on robust self-assembled pseudorotaxane systems, in which 24-crown-8 and secondary dialkylammonium are selected as binding motifs and anthracene at the wheel and naphthalenediimide (NDI) in the axle as two matching rigid spacers.[12] Herein, we synthesized a [3]rotaxane (**3**) and a pH-controlled bistable [3]rotaxane (**4**) with an electron-rich pyrene moiety at the wheel and an electron-deficient NDI unit in the middle of the axle through "click chemistry". Different from those reported bistable [3]rotaxanes or [4]rotaxanes in which the charge-transfer behavior was controlled by the redox states between donor and acceptor,[7b,11d] the present bistable [3]rotaxane **4** displays an intramolecular charge-transfer (ICT) process controlled by the spacial distance of the pyrene moiety with the NDI.

The synthesis of the [3]rotaxanes **3** and **4** is depicted in Scheme 1. The template-directed synthesis of rotaxane and catenanes by click chemistry (Cu^{I}-catalyzed Huisgen 1,3-dipolor cycloadditions between azides and alkynes) is an effective method for end-blocking of these systems.[13] The crown ether macrocycle **2** was synthesized in 50% yield by treating 4-hydroxymethyldibenzo-24-crown-8 with 1-pyrenebutyric acid in the presence of *N*,*N*′-dicyclohexylcarbodiimide (DCC) and 4-dimethylaminopyridine (DMAP) (Scheme S3, Supporting Information). The [3]rotaxane **3** was prepared in 11% yield by adding 3,5-di(*tert*-butyl)benzyl azide to a CH_3CN solution of the bis(ammonium) rod **1** (Scheme S2, Supporting Information) and **2** via click chemistry. Finally, the N-methylation of two triazoles in **3** and the subsequent salt exchange gave **4** in 75% yield.

To demonstate the importance of the stopper in **3** and **4** for controlling the ICT behavior between the wheel and the axle, we first performed the UV/vis absorption spectroscopy experiments of the resultant pseudorotaxane of **1** with **2** (Figure S14, Supporting Information). When 2 equiv of **2** was added to the CH_3CN solution of **1**, the color of the solution changes from slightly green to red. This is a result of the charge transfer (CT) between the pyrene moiety and the NDI unit. In the controlled experiments, the color change was hardly observed upon addition of **2** to the $CH_3CN/CHCl_3$ (1:1) solution of the axis molecules **5/6** (Figure S17, Supporting Information). In addition, comparing the ^1H NMR spectra of the mixed solution of **2** and **1** with only the wheel molecule **2** and the corresponding axis molecule **1** (Figure S18, Supporting Information), we can validate that the macrocycles 24-crown-8 locate at the ammonium of the aliphatic chain of **1**. These observations confirm the formation of a pseudorotaxane between **1** and **2**. Furthermore, upon addition of 2 equiv of Et_3N, the red solution of the

Scheme 1. Synthesis of the [3]Rotaxanes **3** and **4** and the Structures of the Axis Molecules **5** and **6**

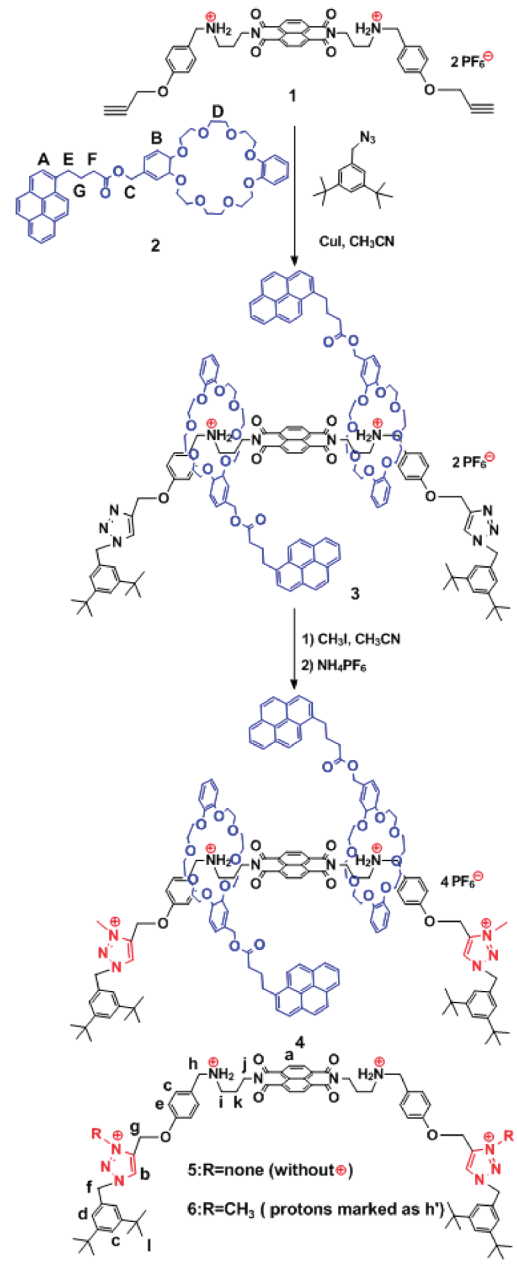

(6) (a) Altieri, A.; Bottari, G.; Dehez, F.; Leigh, D. A.; Wong, J. K. Y.; Zerbetto, F. *Angew. Chem., Int. Ed.* **2003**, *42*, 2296–2300. (b) Saha, S.; Flood, A. H.; Stoddart, J. F.; Impellizzeri, S.; Slivi, S.; Venturi, M.; Credi, A. *J. Am. Chem. Soc.* **2007**, *129*, 12159–12171. (c) Coskun, A.; Friedman, D. C.; Li, H.; Patel, K.; Khatib, H. A.; Stoddart, J. F. *J. Am. Chem. Soc.* **2009**, *131*, 2493–2495.

(7) (a) Jiménez, M. C.; Dietrich-Buchecker, C.; Sauvage, J.-P. *Angew. Chem., Int. Ed.* **2000**, *39*, 3284–3287. (b) Liu, Y.; Flood, A. H.; Bonvallet, P. A.; Vignon, S. A.; Northrop, B. H.; Tseng, H.-R.; Jeppesen, J. O.; Huang, T. J.; Brough, B.; Baller, M.; Magonov, S.; Solares, S. D.; Goddard, W. A.; Ho, C.-M.; Stoddart, J. F. *J. Am. Chem. Soc.* **2005**, *127*, 9745–9759.

(8) Badjic, J. D.; Ronconi, C. M.; Stoddart, J. F.; Balzani, V.; Silvi, S.; Credi, A. *J. Am. Chem. Soc.* **2006**, *128*, 1489–1499.

(9) (a) Sauvage, J.-P. *Acc. Chem. Res.* **1998**, *31*, 611–619. (b) Schalley, C. A.; Beizai, K.; Vögtle, F. *Acc. Chem. Res.* **2001**, *34*, 465–476.

(10) Serreli, V.; Lee, C.-F.; Kay, E. R.; Leigh, D. A. *Nature* **2007**, *445*, 523–527.

(11) (a) Poleschak, I.; Kern, J.-M.; Sauvage, J.-P. *Chem. Commun.* **2004**, 474–476. (b) Raiteri, P.; Bussi, G.; Cucinotta, C. S.; Credi, A.; Stoddart, J. F.; Parrinello, M. *Angew. Chem., Int. Ed.* **2008**, *47*, 3536–3539. (c) Zhao, Y.-L.; Aprahamian, I.; Trabolsi, A.; Erina, N.; Stoddart, J. F. *J. Am. Chem. Soc.* **2008**, *130*, 6348–6350. (d) Aprahamian, I.; Olsen, J.-C.; Trabolsi, A.; Stoddart, J. F. *Chem.—Eur. J.* **2008**, *14*, 3889–3895.

(12) Jiang, W.; Han, M.; Zhang, H.-Y.; Zhang, Z.-J.; Liu, Y. *Chem.—Eur. J.* **2009**, *15*, 9938–9945.

(13) Miljanì, O.Š.; Dichtel, W. R.; Aprahamiana, I.; Rohde, R. D.; Agnew, H. D.; Heath, J. R.; Stoddart, J. F. *QSAR Comb. Sci.* **2007**, *26*, 1165–1174.

pseudorotaxane turned light red and the absorption band at about 516 nm decreased, indicating that the pseudorotaxane gradually disassociated.

Similar to the above pseudorotaxane, there is also a CT band at about 525 nm for **3** and 520 nm for **4**, indicating that the ICT process occurs between the pyrene moiety and the NDI unit. Interestingly, when 2 equiv of phosphazene base P_1-*t*-Bu (PBB) was added to the solution of **3** or **4**, the intensity of the ICT bands does not decrease, but increases, as shown in Figure 1. The addition of CF_3COOH again

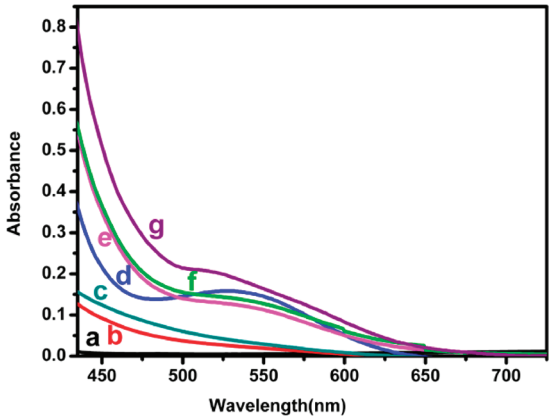

Figure 1. Absorption spectra of (a) the wheel molecule **2** (2 mM), (b) the axle molecule **5** (1 mM), (c) the axle molecule **6** (1 mM), (d) [3]rotaxane **3** (1 mM), (e) [3]rotaxane **4** (1 mM), (f) **4** (1 mM) + PBB (2 mM) + CF_3COOH (4 mM), and (g) **4** (1 mM) + PBB (2 mM) in $CH_3CN/CHCl_3$ = 1:1.

decreases the CT band. One reasonable explanation for the enhancement of the absorption is that the spacial distance between the pyrene moiety and NDI in **3/4** is an important factor for their interaction.

Quantitative analyses on the CT band can provide more information to evaluate the nature of the CT state. The feature of the CT absorption band can been related to the Marcus−Hush electronic coupling element H_{DA} between the donor and acceptor units involved in the charge-transfer transition. As can been seen from Table 1, the values of H_{DA} increase in the order of $H_{DA(4)} < H_{DA(4+PBB+CF_3COOH)} < H_{DA(4+PBB)}$. That is, the charge-transfer transition ability of the donor−acceptor

Table 1. UV−Vis Absorption and Luminescence Properties of the [3]Rotaxanes

compound	$H_{DA}(cm^{-1})^a$	Φ (%)^b	τ (ns)^c
2		12.72	18.63
3	2176	2.00	17.32
4	1930	3.95	18.46
4 + PBB	3493	2.85	18.50
4 + PBB + CF_3COOH	2019	3.36	18.42

[a] Donor−acceptor electronic coupling element and its values are taken from Table S1 (Supporting Information). [b] Luminescence quantum yield. [c] Lifetime.

pairs in **4** is the strongest in the presence of PBB, and that is the weakest in the absence of both acid and base. This supports the changes on the CT bands in Figure 1.

The luminescence properties of the two pyrene units in the [3]rotaxane systems give further insights of the complexation behaviors. The absence of the excimer peak in **3** and **4** implies that the two pyrene units cannot interact by $\pi-\pi$ stacking (Figure S21, Supporting Information). Interestingly, the fluorescence intensity of **4** (Φ = 2.85%) decreases upon addition of PBB to the solution of **4** (Φ = 3.95%) and increases again upon further addition of CF_3COOH (Φ = 3.36%) (Figure S22, Supporting Information). The measurement of the fluorescence lifetimes shows that there is only a lifetime for **2**, **3**, **4**, **4** + PBB, and **4** + PBB + CF_3COOH, and all values obtained are in the scope of the error of the instrument (Table 1). These observations suggest that the charge transfer excited state in the [3]rotaxane systems should be nonfluorescent,[14] and the luminescence in different systems comes from the free pyrene moiety. That is to say, only one pyrene forms the CT complex, while the other one may not stack with the NDI unit.

To obtain in-depth mechanistic insight into the unusual photophysical behavior, we performed ^1H NMR experiments of **4**. As can be seen from Figure S12, there is an obvious downfield shift for H_h ($\Delta\delta$ = 0.26 ppm) and H_i ($\Delta\delta$ = 0.18 ppm) in **4** relative to H_h and H_i in free **6**. On the other hand, the chemical shifts of H_d, H_f, H_b, and $H_{h'}$ are almost unchanged. These observations suggest that DB24C8 in **4** is mostly located at the secondary *N*-alkylanilinium position and not the triazolium group.[15] On the basis of the change of integrated area of the protons in NDI (H_a), we deduced that the resonances of H_a split into two equal parts: $H_{a'}$ at the original position and other peak(s) overlapped with H_A or H_B. This means that not all of the protons in NDI participate in the formation of the CT complex with the pyrene moiety. In addition, the resonances of H_A in pyrene also exhibit obvious upfield shifts. This should be attributed to partial $\pi-\pi$ stacking between the pyrene of **2** and the NDI of **6**, due to their mutual shielding/deshielding effects.[16] Therefore, the ICT process occurs between the electron-rich donor (pyrene) and the electron-deficient acceptor (NDI).

Upon the addition of 2.0 equiv of PBB to the solution of **4**, the signals of protons H_h, H_i, H_f, and $H_{h'}$ shift upfield, while that of H_b ($\Delta\delta$ = 0.8 ppm) exhibits downfield shift (Figure 2). These combined observations suggest that the DB24C8 moieties move from the secondary *N*-alkylanilinium to the triazolium groups. It is noted that the peak of $H_{a'}$ is completely absent, which indicates that all of the protons in NDI participate in the formation of the CT complex with the pyrene moiety, and results in the comfortable $\pi-\pi$ stacking between the electron donor and acceptor pairs.

(14) Hamilton, D. G.; Davies, J. E.; Prodi, L.; Sanders, J. K. M. *Chem.—Eur. J.* **1998**, *4*, 608–620.
(15) (a) Coutrot, F.; Busseron, E. *Chem.—Eur. J.* **2008**, *14*, 4784–4787. (b) Coutrot, F.; Romuald, C.; Busseron, E. *Org. Lett.* **2008**, *10*, 3741–3744.
(16) (a) Colquhoun, H. M.; Zhu, Z.; Williams, D. J. *Org. Lett.* **2003**, *5*, 4353–4356. (b) Colquhoun, H. M.; Zhu, Z.; Cardin, C. J.; Gan, Y. *Chem. Commun.* **2004**, 2650–2652. (c) Colquhoun, H. M.; Zhu, Z. *Angew. Chem., Int. Ed.* **2004**, *43*, 5040–5045.

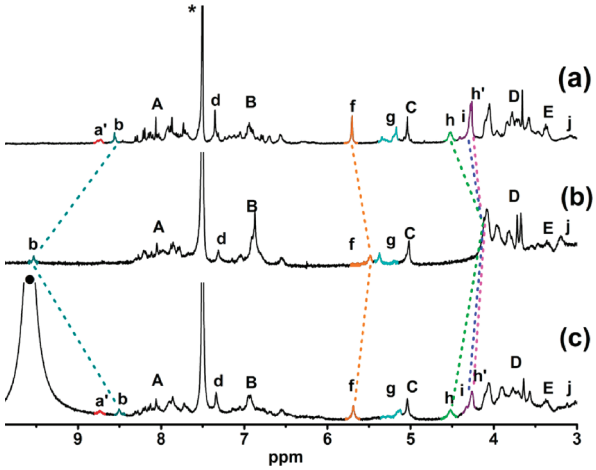

Figure 2. ^{1}H NMR spectra (400 MHz, $CD_3CN/CDCl_3$ = 1:1, 298 K) of (a) **4** (1 mM), (b) **4** (1 mM) + PBB (2 mM), and (c) **4** (1 mM) + PBB (2 mM) + CF_3COOH (4 mM); ●, peak of CF_3COOH; ∗, peak of $CDCl_3$).

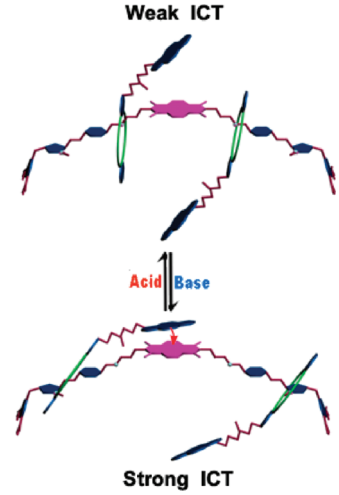

Figure 3. Schematic representation of the mode for the base−acid-controlled ICT behavior in [3]rotaxane **4**.

Hence, the increase of the absorption spectrum at about 520 nm is a natural process. As expected, when 4.0 equiv of CF_3COOH was added to the above solution, the peaks of H_h, H_i, H_f, $H_{h'}$, and H_b return to their original positions (Figure 2c). This means that DB24C8 shuttles again to the secondary *N*-alkylanilinium position, accompanying the decrease of the absorption spectrum at about 520 nm. We also carried out the molecular energy minimization on the system (Figure S20, Supporting Information) to compare the distance of pyrene with NDI in **4** in the absence and presence of PBB. The calculation results indicate that the distance between pyrene and NDI in the absence of PBB is larger than that in the presence of PBB. This explains the above observations on the ICT change. On the basis of all the above discussions, the schematic representation of the mode for the base−acid-controlled ICT behavior in [3]rotaxane **4** is illustrated in Figure 3.

In conclusion, two [3]rotaxanes **3** and **4** have been synthesized via click chemistry, and the photophysical behavior of **4** upon addition of base and acid has been investigated. In neutral conditions, the DB24C8 moieties are located at the ammonium of the aliphatic chain of the wheel, and a weaker CT band appears due to the interaction of the pyrene moiety with the NDI unit. Addition of base leads to the movement of the DB24C8 moieties from the secondary *N*-alkylanilinium to the triazolium groups and accompanies efficient enhancement of the ICT intensity. This bistable [3]rotaxane represents a new prototype of performing photophysical function by adjusting the spacial distance between donor and acceptor in mechanically interlocked molecules.

Acknowledgment. This work was supported by 973 Program (2006CB932900), NNSFC (Nos. 20932004, 20772063 and 20972077).

Supporting Information Available: Synthesis of compounds, UV−vis, NMR, fluorescence spectra, and computational modeling procedures. This material is available free of charge via the Internet at http://pubs.acs.org.

OL100321K